SPACE TELESCOPE SCIENCE INSTITUTE
Operated for NASA by AURA

COS Instrument Science Report 2010-05(v1)

SMOV: COS NUV Wavelength Calibration

Cristina Oliveira, Stéphane Béland, Charles (Tony) Keyes, & Sami Niemi
February 19, 2010

ABSTRACT

COS calibration program 11474 was carried out during SMOV to characterize the wavelength scales of the NUV detector. Science data were obtained with the G185M, G225M, G285M, and G230L gratings through the Primary Science Aperture (PSA), simultaneously with PTNe lamp line data, obtained through the Wavelength Calibration Aperture (WCA). These data were partially calibrated with the COS pipeline and then, in conjunction with STIS data of the same target, used to derive offsets between the PSA and WCA wavelength scales. These offsets are then used to place the dispersion relations derived from thermal vacuum 2003 (TV03) in the on-orbit frame of reference, so that correct wavelengths can be assigned to the on-orbit COS data.

Contents:

1. Introduction

The COS NUV channel contains one low resolution (G230L) and three medium resolution (G185M, G225M, and G285M) gratings, providing wavelength coverage from 1670 to 3560 Å. Spectra of external targets are obtained through the Primary Science Aperture (PSA) while wavelength calibration spectra are obtained through the Wavelength Calibration Aperture (WCA). There are two PtNe line lamps on-board, and wavecal data can be obtained concurrently with science data (TAGFLASH mode) or either before or after a science exposure is obtained. Wavecal data is used by the COS pipeline (CalCOS) to correct for any offsets between the wavecals and the lamp template reference files due to non-repeatability in the grating mechanism positions. These offsets are then applied to the science data as well, before wavelengths are assigned (COS Data Handbook; Shaw et al. 2009)

During thermal vacuum 2003 (TV03) science (PSA) and wavecal (WCA) data were obtained at all central wavelengths of the NUV gratings, using an internal and an external PtNe line lamp. These data were used to derive dispersion relations for all the NUV modes (for FP-POS = 3 only), by cross-correlating the observed spectra, in pixel space, with a PtNe wavelength line list. A second order dispersion relation was used for all the NUV gratings. Because of the different optical paths between the PSA and WCA, the dispersion relations derived for each aperture are different. The dispersion solutions for the PSA are not adequately represented by a simple offset of the WCA dispersion solutions. A separate dispersion solution is needed for each stripe, for each central wavelength of each grating, for each aperture. Because the WCA and PSA have different dispersion solutions we cannot use WCA data obtained on-orbit to determine directly the on-orbit dispersion solutions for the PSA. Instead we use the PSA dispersion solutions derived from TV03 data to wavelength calibrate PSA data obtained on-orbit. However, the TV03 dispersion solutions cannot be directly applied to on-orbit data without placing the TV03 dispersion solutions on the on-orbit frame of reference, which implies deriving the on-orbit offsets between the PSA and WCA spectra, as described below.

Program 11474 was executed during SMOV to obtain spectra of external targets, that would allow us to determine the on-orbit offsets between the PSA and WCA data. Together with data from program 11475, these offsets are then used to place the dispersion relations derived in TV03 in the on-orbit frame of reference, so that correct wavelengths can be assigned to the on-orbit COS data, using the TV03-derived dispersion coefficients. As a first approximation, we determine an average value, constant in wavelength for each setting, for the offsets between the PSA and WCA apertures. Future refinements to the NUV wavelength calibration will take into account the second order effect resulting from the fact that the PSA and WCA dispersion solutions are different, and so the offsets between the PSA and WCA are wavelength dependent.

Program 11475, a companion program to program 11474, was executed during SMOV with the purpose of obtaining wavelength calibration spectra through the WCA at all FP-POS, for all the central wavelengths of the NUV gratings, so that the lamp

template reference file can be updated to the on-orbit frame of reference.

2. Observations

Data for the wavelength calibration of the NUV detector were obtained in program 11474 (COS NUV Internal/External Wavelength Scales). Table 1 summarizes the exposures taken in the different visits of this program. All the visits used a NUV target acquisition sequence consisting of ACQ/SEARCH (SCAN-SIZE=5 or 4; STEP-SIZE=1.767), followed by ACQ/SEARCH (SCAN-SIZE=2; STEP-SIZE=1.767), ACQ/PEAKXD, and ACQ/PEAKD (NUM-POS=9; STEP-SIZE=1.0) to achieve maximum centering accuracy. The optical element used for target acquisition is the first one given in Table 1, for each visit. All the exposures (except for G285M/2979 and G285M/3035 in Visit 01; see below) were obtained in TIME-TAG mode and used special lamp flash parameters (available in ENG mode only) to ensure that multiple flashes were present in each exposure (particularly for the longer exposures), so that any mechanism drift, if at all present, could be easily corrected. The only exposures obtained in program 11474 with G285M/2979/PSA (180 sec) and G285M/3035/PSA (20 sec) were obtained in Visit 01, and in ACCUM mode (these high count rate exposures were also used to test the response of the NUV detector to high count rates). Each of these ACCUM exposures was immediately followed by a WAVECAL exposure, to allow corrections by the pipeline for mechanism position uncertainties. However, these exposures were short enough that there should not be any drift during the exposure (these exposures are not very different from TIME-TAG exposures where only 1 lampflash is present).

Visit 01 observed HD 187691 (F8V), a CORAVEL radial velocity standard (Udry et al. 1999), with $v_{\rm rad} = 0.0 \pm 0.3$ km/s, which has also been observed by STIS (E230M, 0.2x0.06, exposure o52601020, covering [2274,3118] Å). Visit 02 observed another radial velocity standard, HD 6655 (F8V), which has $v_{\rm rad}$ = 19.5 $\pm$ 0.3 km/s. Visit 03 observed NGC 6833, a slightly extended PN (0.2 arcsec), for which the radial velocity is also known ($-$108.8 m/s). Visits 70 and 74 observed Feige 48, a rapidly pulsating subdwarf B (sdB) star with an unseen companion. This star has a pulsating period of 344–379 sec (Koen et al., 1998) and a rotation period of 0.376 ± 0.003d with a velocity semi-amplitude of 28.0 ± 0.2 km/s (O'Toole, Heber, & Benjamin, 2004). Feige 48 has also been observed by STIS, both with the E140M and E230M gratings (E230M, 0.2x0.06, exposure o64002030, covering [1606,2366] Å).

As part of the updating of the NUV wavelength scales, lamp template data was also obtained. Program 11475 (COS Internal NUV Wavelength Verification) obtained internal wavelength calibration spectra using the default PtNe lamp (Lamp 1) with each NUV grating, at each central wavelength setting, and for each FP-POS position. Each exposure had a duration of 120 sec (some exposures were 150 sec). In order to allow the mechanism drift to settle after a grating motion, a 1800 sec exposure (containing multiple flashes of the lamp) was taken at the beginning of each visit. Analysis and results of the mechanism drift monitoring exposures will be presented in another ISR.

3. Data Analysis

To assess the impact of mechanism drift in the wavecal exposures obtained in program 11475, each exposure was divided in 30 sec time slices, for each stripe, and each time slice was cross-correlated with the first time slice. The maximum drift for any wavecal exposure was 0.9 pixel, with most drifts smaller than 0.3 pixels. The drifts found are all much smaller than the resolution element of 3 pixels, and so no drift correction was applied to the wavecal exposures.

The wavecal data were extracted into 1d spectra (counts vs pixel) and then the 1d spectra were used to produce a new NUV lamp template reference file, containing one entry per FP-POS for each grating/cenwave/stripe combination. In addition, each of the 1d spectra corresponding to FP-POS = 3 was cross-correlated with the 1d spectra for the same grating/cenwave/stripe mode and FP-POS = 3 in the TV03-based lamp template reference file, in order to determine their separation, $\mathrm{WCA_{TV03}}$ - $\mathrm{WCA_{SMOV}}$. This value is needed so that the wavelength calibration is performed properly, as all the wavecal data obtained on-orbit is compared with a lamp template reference file that was also updated from on-orbit data. In addition, since the dispersion solutions from TV03, which are applied to the on-orbit data, and the lamp template reference file for TV03 are only for the FP-POS = 3 position, the separation between the $\mathrm{WCA_{TV03}}$ - $\mathrm{WCA_{SMOV}}$ for other FP-POS is not necessary (see below).

3.1 HD 187691 and HD 6655

The rawtag files for each of the science exposures obtained in Visit 01 and Visit 02 of program 11474 were partially calibrated with CalCOS by setting all the calibration switches to *OMIT* except for *DOPPCORR* and *WAVECORR*, which were set to *PERFORM*. The new lamp template reference file, described above, was used in this calibration, so that the exposures are placed in the on-orbit frame of reference. To produce 1d science and wavecal spectra, the *xfull* and *yfull* columns of the resulting corrtag files, which are corrected for doppler smearing and mechanism drift for the science spectra, and for mechanism drift for the wavecal spectra, were extracted using *Cedar*,, each stripe independently, using the default extraction paramenters used by CalCOS.. The resulting 1d files contain then counts vs pixel.

The heliocentric correction is only applied by the pipeline when wavelengths are being assigned. Since our analysis of the science data was done in pixel space, this correction was not applied. However, since for all the exposures analyzed here $|v_{\mathrm{Helio}}| \leq 2$ km/s this effect is less than 0.5 pixels for both the M and L gratings.

The on-orbit separation, in pixels, between each stripe of the PSA and WCA data, was determined by first cross-correlating the 1d WCA spectra with a PtNe line list, so that wavelengths can be assigned to each of the PtNe emission lines seen in pixel space. Each emission line, i, has then a pixel coordinate, $\mathrm{WCA_{SMOV,i}}$.

The next step is to identify the pixel positions in the 1d PSA spectra, corre-

sponding to the wavelengths of the PtNe emission lines, identified in the previous step, $PSA_{SMOV,i}$. In the case of data obtained in Vis 01 for HD 187691 this was accomplished by using the STIS/E230M spectrum of this target. For each feature corresponding to the wavelength being considered, the STIS spectrum was used as a guide, so that the pixel position of the same feature could be looked up in pixel space, in the 1d PSA COS spectrum. For each grating/cenwave/stripe this procedure was applied to as many features as possible so that one can determine $PSA_{SMOV,i}$ - $WCA_{SMOV,i}$ across the detector. The on-orbit separation between the PSA and WCA data is then calculated, for each grating/cenwave/stripe, by calculating the mean of ($PSA_{SMOV,i}$ - $WCA_{SMOV,i}$) = PSA_{SMOV} - WCA_{SMOV}.

HD 6655, observed in Visit 02 of program 11474, has not been observed by STIS, and so this procedure cannot be applied as described above. However, since HD 6655 and HD 187691 have the same spectral type, and both have accurately known radial velocities, one can simulate the STIS spectrum of HD 6655 by using the STIS spectrum of HD 187691 and taking both of the radial velocities into account. The simulated HD 655 STIS spectrum can then be used to derive PSA_{SMOV_i}, as described above.

Table 2 summarizes the different measurements using data obtained in Vis 01 and 02 of program 11474. For each grating and cenwave, columns 3 through 5, contain for each stripe, first the mean of ($PSA_{SMOV,i}$ - $WCA_{SMOV,i}$) (for most modes, between 3 and 5 measurements were used to determine this mean) and then the separation between the TV03 and on-orbit lamp templates, WCA_{TV03} - WCA_{SMOV}, discussed above. The column "Notes" indicates which data was used. There are some cases for which there is no overlap between the COS and STIS data, and so $PSA_{SMOV,i}$ - $WCA_{SMOV,i}$ could not be measured; these are labeled as "no overlap". There are also some cases, labeled "no wavecal", for which the lamp spectrum taken concurrently with the science spectrum (TAGFLASH) yielded very few lamp counts and so $WCA_{SMOV,i}$ could not be measured. These exposures will have to be repeated in the future. Note that for the 2695 cenwave of the G285M grating, the encoder position was adjusted during SMOV, hence the large values of WCA_{TV03} - WCA_{SMOV} for each stripe, in Table 2. Note also that for stripes where colum 6 of Table 2 contain '...' the wavelength dispersion reference file was not updated. Table 3 gives the rootnames of the exposures used to measure the PSA to WCA offsets presented in Table 2.

Stripe A of G230L/2635 covers the wavelength range 1334–1733 Å. The combination of the very low NUV detector's sensitivity at these wavelengths together with a substantial decrease in the flux of F8V stars at these wavelengths, leads to a spectrum with very low S/N and without any apparent features, making it impossible to determine $PSA_{SMOV,i}$ for this case. This is indicated in Table 2 as "low S/N". A similar effect is seen in stripe C of the G230L grating, which sees 2nd order light, for all the cenwaves. G230L/2635/C, G230L/2950/C, and G230L/3000/C cover 1768–1967 Å, 1900–2100 Å, and 1950–2150 Å, respectively (second order), and at these wavelengths the fluxes of our target are too low to get a good S/N in a 60 sec exposure time. The low S/N with no apparent features makes it impossible to measure $PSA_{SMOV,i}$ for these cases as well

(even if the spectra were of adequate S/N, there is no overlap with the existing STIS data of HD 187691). For G230L/3360/C, covering 2164–2361 Å, the PSA spectrum has adequate S/N, but the wavecal spectrum has very little counts and so we cannot determine $WCA_{SMOV,i}$ (marked in the table as "no wavecal").

3.2 Feige 48 add NGC 6833

Feige 48 is our primary calibration target for the G185M grating. As mentioned above, this target has also been observed by STIS and a technique similar to that used with HD 187691 will be used with this target to derive $PSA_{SMOV,i}$ - $WCA_{SMOV,i}$ for the G185M grating. However, before this analysis can begin, the Feige 48 spectra need to be first corrected for the orbital motion. We are currently in the process of determining whether we can reliably remove the orbital motion from both the STIS and COS data and use the Feige 48 data for G185M wavelength calibration.

The analysis of NGC 6833 also requires some care - since this is a slightly extended source the extraction of the 1d spectra has to be done in a special way to minimize the contamination of the emission profiles by the extended part. This target is used as a confirmation of the wavelength scales, and not as a primary target, as there is no other independent source to confirm the wavelengths seen in the COS data (as done for HD 187691 with STIS data). In addition, for emission lines produced by known species and for which the wavelengths can be calculated by taking the nebula radial velocity into account, there is still some uncertainty in those wavelengths, given that the emission lines are typically broad and their centroid can be influenced by how the 1d extraction was performed.

3.3 Wavelength Calibration in CalCOS

Program 11474 was executed during SMOV to obtain spectra of external targets, that would allow us to determine the on-orbit offsets between the PSA and WCA data. Together with data from program 11475, these offsets are then used to place the dispersion relations derived in TV03 in the on-orbit frame of reference, so that correct wavelengths can be assigned to the on-orbit COS data, using the TV03-derived dispersion coefficients for the PSA.

Wavelength calibration by the COS pipeline is described in detail in the *COS Data Handbook* (Shaw et al. 2009), here we only present a summary.

The COS pipeline determines the dispersion-direction shift that needs to apply to the science data (PSA) to correct shifts due to the non-repeatability of the OSM mechanism by comparing the wavecal data (WCA) obtained concurrently (if in tagflash mode) with the data contained in the lamp template reference file. This reference file contains one entry per FP-POS for each of the available modes, and so the wavecal data is compared with the lamp data at the same FP-POS. The lamp template reference file contains also a column that gives the separation in pixels between the lamp template

at FP-POS = 3 and the lamp templates at the other FP-POS. The shift determined by comparing the wavecal data to the lamp plus the shift read from the column of the lamp template reference file are applied to the data, producing the $xfull$ pixel coordinate.

The COS pipeline computes then the wavelength from the xfull pixel coordinate, $xfull$, as $xprime = xfull + d_{\rm PSA}$, where $d_{\rm PSA} = d_{\rm TV03} - d$. $d_{\rm TV03}$ is the separation between the PSA and WCA data in TV03, $\rm PSA_{TV03}$ - $\rm WCA_{TV03}$, and d is the separation between the PSA and WCA data on-orbit (SMOV), taking into account that the WCA data in SMOV is offset from the WCA in TV03: d = $\rm PSA_{SMOV}$ - $\rm WCA_{SMOV}$ - ($\rm WCA_{TV03}$ - $\rm WCA_{SMOV}$). The wavelengths are then computed from $\lambda = a_0 + a_1 \times xprime + a_2 \times xprime^2$, where a_0, a_1, and a_2 are the dispersion coefficients derived from TV03 data. Each stripe of each grating/cenwave mode has its own dispersion solution.

4. Results

The offsets presented in column 6 of Table 2, d, were used to update the NUV wavelength dispersion reference file (except for the stripes marked with '...' in column 6; these settings will use the thermal vacuum values). This updated reference file was then used to process COS data obtained in two SMOV programs (independent of the SMOV wavelength calibration programs), so that the accuracy of the wavelength scales can be determined.

Visit 01 of COS program 11477 (COS NUV External Spectroscopic Performance - Part 2) observed the symbiotic star AG Draconis, a spatially unresolved point source with an emission line spectrum, on Sep 7 2009. Exposure labm01eeq was obtained with G225M/2390 at FP-POS=3 (TAGFLASH, 110 sec); exposure labm01dqq was obtained with G285M/2739 also at FP-POS=3 (TAGFLASH, 70 sec). AG Draconis has been previously observed by STIS with the E230M grating (exposure o6ky01030, obtained with the 0.2x0.2 aperture and 2707 cenwave; 374 sec) and so the STIS observations can be used to compare the STIS wavelength scales to those of COS.

The two COS exposures of AG Draconis were calibrated with CalCOS (version 2.11f) by setting all the calibration switches to *PERFORM* except for *STATFLAG* and *TDSCORR* which were set to *OMIT*. The resulting spectra, where then compared with the STIS spectra of AG Draconis, which were retrieved from the MAST archive. No convolution of the STIS data, with the COS LSF, was performed. Data with intrinsically broad lines was used to evaluate the G225M and G285M wavelength scales; in the case of G230L, the STIS data used for the comparison of the wavelength scales is of poorer resolution.

Figure 1 shows one wavelength region for each of the three COS stripes of the G225M/2390 AG Draconis observation. Overplotted in red in the STIS/E230M spectrum of this target. There is good agreement between the COS and STIS wavelengths for stripes A and B, for stripe C the COS wavelengths are under-predicted by $\sim$2 pixels.

Figure 2 shows one wavelength region for each of the three COS stripes of the G285M/2739 AG Draconis observation (in black), again with the STIS/E230M spectrum of this target overplotted in red. For both stripes A and C the COS wavelengths are over-predicted by $\sim$1 pixel, while for stripe B the COS wavelengths are under-predicted by $\sim$1 pixel.

To evaluate the G230L wavelength scales we used COS data of AzV 18, observed in program 11472 (COS NUV Dispersed-light Acquisition Algorithm Verification), with the G230L/2950/FP-POS=3 setup (exposure laa004p1q, observed in TIME-TAG mode for 60 sec on Aug 11, 2009). This target has also been observed by STIS, with the G230LB grating, through the 52x2 aperture (exposure o6df06010). Even though the G230LB grating is of lower resolution than the G230L grating, comparing the two spectra is still useful to evaluate the G230L wavelength scales.

Figure 3 displays the Mg II $\lambda\lambda$ 2796, 2803, and Mg I λ 2852 regions in the COS observation of AzV 18 (G230L/2950/stripe B, in black), with the STIS/G230LB spectrum overplotted in red. For this stripe the COS wavelengths are under-predicted by $\sim$1–2 pixels.

Even though the figures presented here seem to indicate that the accuracy of the wavelength scales is within the specifications defined in Table 4 (except for the G185M wavelength scales which have not been updated yet), the limited number of datasets on which the updated wavelength scales have been tested makes any conclusions preliminary. More work is required to further refine our evaluation of the NUV wavelength scales, in the future. This is discussed below.

5. Reference Files Delivered

As a result of the work described in this ISR the reference files below were delivered to CDBS for use in COS on-the-fly reprocessing (OTFR) on January 29, 2010. Calibrated data obtained from the archive after this date will use these updated reference files (as long as the data were obtained after the USEAFTER date of each file). The files are: u1t1616ol_lamp.fits (NUV lamp template reference file; USEAFTER= 'July 28 2009 00:00:00') and u1t1616pl_disp.fits (FUV wavelength calibration reference file; USEAFTER= 'July 28 2009 00:00:00'). Note that for entries marked as '...' in column 6 of Table 2 no updates have been made to the wavelength dispersion reference file, i.e., the thermal vacuum values will be the ones used for these settings.

6. Future Work

- Feige 48 and NGC 6833 data obtained in program 11474 will be analyzed in the near future and the results from these analyses will be published.
- Dispersion solutions will be derived for the WCA aperture, using the data obtained in program 11488; they will then be compared to the wavelength dispersion solutions

derived in TV03 for this aperture, in order to determine if they are the same (minus a small offset in pixels).
- A Cycle 17 calibration program (11900) is in place to monitor the stability of the offsets between the PSA and WCA wavelength scales. This calibration program observes HD 187691 and HD 6655 using a subset of cenwaves for each of these NUV gratings.
- STIS data of HD 187691 will be obtained in the Cycle 17 calibration program, so that offsets can be measured for the grating/cenwave/stripe settings marked as “no overlap” in Table 2.
- STIS data of HD 6655, which is our primary standard for the G230L grating, will be obtained in the Cycle 17 calibration program.
- To better evaluate the accuracy of the NUV wavelength scales the current database of SMOV, GTO, and GO observations will be searched for datasets, so that testing of the wavelength scales derived from program 11474 can continue.

7. Change History for COS ISR 2010-05

Version 1: 19 February 2010 - Original Document

References

Shaw, B. et al. 2009, ”COS Data Handbook”, Version 1.0, (Baltimore: STScI).
Koen, C., Donoghue, D. O., Pollaco, D. L., & Nita, A., 1998, MNRAS, 300, 1105
O’Toole, S. J., Heber, U., & Benjamin, R. A., 2004, A&A, 422, 1053
Udry, S., Mayor, M., Maurice E., Andersen, J., Imbert M., Lindgren, H., Mermilliod J. C., Nordstrom B., and Prevot, L., 1999, ASP Conference Series #185, IAU Colloquium 170. Eds. J. B. Hearnshaw and C. D. Scarfe

Table 1. Wavelength calibration exposures in program 11474

Visit	Target	Grating	Cenwave	FP-POS	Visit	Target	Grating	Cenwave	FP-POS
01	HD 187691	G285M	2676	1,2,3,4	03	NGC 6833	G185M	1913	3
...	...	...	2617	3	...	...	...	1921	3
...	...	...	2637	3	...	...	...	2010	3
...	...	...	2657	3	...	...	G225M	2217	3
...	...	...	2695	3	...	...	...	2233	3
...	...	...	2709	3	...	...	...	2325	3
...	...	...	2979	3	...	...	...	2339	3
...	...	...	2850	3	...	...	...	2357	3
...	...	...	3035	3	...	...	...	2373	3
...	...	...	3057	3	...	...	...	2410	3
...	...	...	3074	3	...	...	G230L	2635	3
...	...	...	3094	3	...	...	...	2950	3
...	...	G225M	2250	1,2,3,4	...	...	...	3000	3
...	...	...	2186	3	...	...	...	3360	3
...	...	...	2217	3	...	...	G285M	2676	3
...	...	...	2233	3	70	Feige 48	G185M	1850	3
...	...	...	2268	3	...	...	G285M	2695	3
...	...	...	2283	3	...	...	G225M	2250	3
...	...	...	2306	3	...	...	G230L	2950	3
...	...	...	2325	3	74	Feige 48	G185M	1850	1,2,3,4
...	...	...	2339	3	...	...	...	1786	3
...	...	...	2357	3	...	...	...	1817	3
...	...	...	2373	3	...	...	...	1835	3
...	...	...	2390	3	...	...	...	1864	3
...	...	...	2410	3	...	...	...	1882	3
02	HD 6655	G230L	2950	1,2,3,4	...	...	...	1890	3
...	...	...	2635	3	...	...	...	1900	3
...	...	...	3000	3	...	...	...	1913	3
...	...	...	3360	3	...	...	...	1921	3
...	...	G285M	2850	3	...	...	...	1941	3
...	...	...	2637	3	...	...	...	1953	3
...	...	...	2676	3	...	...	...	1971	3
...	...	...	2695	3	...	...	...	1986	3
...	...	...	2719	3	...	...	...	2010	3
...	...	...	2739	3	...	...	G225M	2250	3
...	...	...	2952	3	...	...	...	2186	3
...	...	...	2996	3	...	...	...	2217	3
...	...	...	3018	3,4	...	...	...	2339	3
03	NGC 6833	G185M	1900	3	...	...	...	2373	3
...	...	...	1817	3	...	...	...	2410	3
...	...	...	1850	3	...	...	...	...	...
...	...	...	1864	3	...	...	...	...	...
...	...	...	1890	3	...	...	...	...	...

Table 2. NUV offsets determined from program 11474

Grating	Cenwave	Stripe A (pixel)	Stripe B (pixel)	Stripe C (pixel)	d (pixel)	Notes
G225M	2186	no overlap, 35.412	no overlap, 35.874	10.296, 36.094	··· , ··· , -25.798	Vis 01
	2217	no overlap, 33.223	no overlap, 33.591	11.910, 33.783	··· , ··· , -21.873	Vis 01
	2233	no overlap, 33.352	no overlap, 33.733	12.379, 33.738	··· , ··· , -21.359	Vis 01
	2250	no overlap, 34.934	no overlap, 35.437	11.607, 35.676	··· , ··· , -24.069	Vis 01
	2268	no overlap, 32.670	9.358, 33.052	9.817, 33.141	··· , -23.694, -23.324	Vis 01
	2283	no overlap, 29.375	9.817, 29.681	12.990, 29.885	··· , -19.864, -16.895	Vis 01
	2306	no overlap, 29.905	11.108, 30.331	14.653, 30.274	··· , -19.223, -15.621	Vis 01
	2325	no overlap, 29.952	11.651, 30.128	14.831, 30.566	··· , -18.477, -15.735	Vis 01
	2339	no overlap, 33.193	12.520, 33.548	13.989, 33.778	··· , -21.028, -19.789	Vis 01
	2357	10.491, 30.857	12.085, 31.175	15.542, 31.462	-20.366, -19.090, -15.920	Vis 01
	2373	9.517, 32.645	12.897, 33.283	16.734, 33.267	-23.128, -20.386, -16.533	Vis 01
	2390	10.172, 32.510	12.661, 33.024	16.801, 33.141	-22.338, -20.363, -16.340	Vis 01
	2410	11.335, 29.070	13.799, 29.420	18.073, 29.467	-17.735, -15.621, -11.394	Vis 01
G285M	2617	3.297, 33.766	5.260, 33.960	9.754, 34.344	-30.469, -28.700, -24.590	Vis 01
	2637	3.948, 35.125	6.405, 35.652	11.178, 35.883	-31.177, -29.247, -24.705	Vis 01
	2657	4.208, 30.183	7.395, 30.546	8.697, 30.664	-25.975, -23.151, -21.967	Vis 01
	2676	4.368, 33.161	6.815, 33.391	10.653, 33.871	-28.793, -26.576, -23.218	Vis 01
	2695[a]	5.019, -106.233	8.827, -108.190	10.631, -110.788	111.252, 117.017, 121.419	Vis 01
	2709	4.913, 34.826	9.043, 35.237	11.110, 35.488	-29.913, -26.194, -24.378	Vis 01
	2719	5.460, 40.373	8.355, 40.900	12.177, 41.262	-34.913, -32.545, -29.083	Vis 02
	2739	4.892, 38.412	9.163, 38.925	9.502, 39.545	-33.520, -29.762, -30.043	Vis 02
	2850	9.286, 35.221	13.093, 35.605	17.505, 35.995	-25.935, -22.512, -18.490	Vis 01
	2952	13.848, 35.923	13.544, 36.721	19.516, 37.043	-22.075, -23.177, -17.527	Vis 02
	2979	-4.795, 35.162	-2.431, 35.521	-0.108, 36.144	-39.957, -37.952, -36.252	Vis 01
	2996	13.177, 36.118	16.058, 36.722	no wavecal, 36.892	-22.941, -20.664, ···	Vis 02
	3018	12.859, 36.425	16.533, 37.312	20.399, 37.645	-23.566, -20.779, -17.246	Vis 02
	3035	-4.186, 36.121	-2.043, 36.645	no overlap, 37.040	-40.307, -38.688, ···	Vis 01
	3057	16.881, 38.474	19.515, 39.584	no wavecal, 40.594	-21.593, -20.069, ···	Vis 01
	3074	16.794, 37.095	20.115, 37.575	no wavecal, 38.455	-20.301, -17.460, ···	Vis 01
	3094	17.264, 37.757	19.944, 38.475	no overlap, 39.149	-20.493, -18.531, ···	Vis 01
G230L	2635	low S/N, -1.81	-40.284, -2.282	low S/N, -3.149	··· , -38.002, ···	Vis 02
	2950	no overlap, 3.083	-38.334, 2.703	low S/N, 1.914	··· , -41.037, ···	Vis 02
	3000	no overlap, 4.576	-39.609, 4.235	low S/N, 3.662	··· , -43.844 , ···	Vis 02
	3360	-40.715, -2.725	no overlap, -3.127	no wavecal, -4.023	-37.990, ··· , ···	Vis 02

Note. — The first number reported in columns 3 through 5 is the mean of ($PSA_{SMOV,i}$ − $WCA_{SMOV,i}$) for each stripe, while the second number is WCA_{TV03} - WCA_{SMOV} for each stripe as well (from analysis of data obtained in program 11475). Entries labeled *no overlap* indicate that the on-orbit separation between the PSA and WCA could not be measured due to lack of overlap between the STIS and COS data. Entries marked *no wavecal* indicate cases for which $WCA_{SMOV,i}$ could not be measured due to very low S/N of the wavecal data, while entries marked *low S/N* indicate cases for which $PSA_{SMOV,i}$ could not be measured because of the low S/N of the science data. Column 6, d, contains PSA_{SMOV} - WCA_{SMOV} - (WCA_{TV03} - WCA_{SMOV}) (in pixels) for stripes A, B, and C, respectively. The last column indicates the source of the data used for the different measurements.

[a]Note that the endocoder position was adjusted during SMOV for this setting, hence the large values of (WCA_{TV03} - WCA_{SMOV}) for each stripe.

Table 3. Exposures used to determine NUV offsets from program 11474

Grating	Cenwave	Exposure	Grating	Cenwave	Exposure
G225M	2186	labq01koq	G285M	2695	labq01jcq
	2217	labq01kqq		2709	labq01jeq
	2233	labq01ksq		2719	labq02n8q
	2250	labq01keq		2739	labq02o1q
	2268	labq01kuq		2850	labq01jkq
	2283	labq01kwq		2952	labq02o3q
	2306	labq01kyq		2979	labq01lgq
	2325	labq01l0q		2996	labq02o5q
	2339	labq01l2q		3018	labq02o9q
	2357	labq01l4q		3035	labq01jqq
	2373	labq01l6q		3057	labq01lkq
	2390	labq01lcq		3074	labq01jyq
	2410	labq01leq		3094	labq01k4q
G285M	2617	labq01izq	G230L	2635	labq02mnq
	2637	labq01j1q		2950	labq02mdq
	2657	labq01jaq		3000	labq02mpq
	2676	labq01i5q		3360	labq02muq

Table 4. COS Specifications for NUV Wavelength Accuracies

Grating	Error Goal (1σ) (km s^{-1})	Error Goal (1σ) (pixels)	Internal Error (pixels)
G185M	15	7.2–10.0	1.2–1.7
G225M	15	9.7–13.3	1.6–2.3
G285M	15	9.7–14.7	1.6–2.6
G230L	175	8.3–15.5	1.4–2.6

Note. — The internal error includes the accuraccy of the wavelength scale, the dispersion relation, aperture offsets, distortions and drifts. The error goal includes contributions from external sources, which are dominated by target mis-centering in the aperture. Error goal given per exposure.

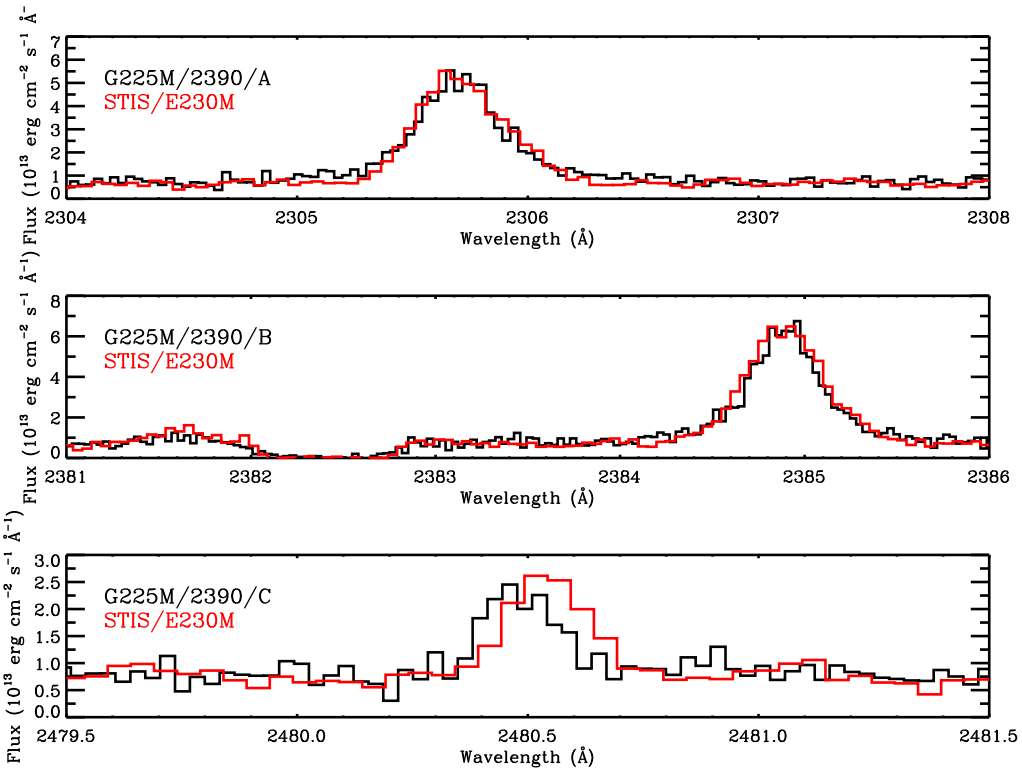

Figure 1. Comparison between STIS/E230M (red) and COS/G225M/2390 (black) wavelength scales using AG DRAC data. COS data is from program 11477, for FP-POS = 3.

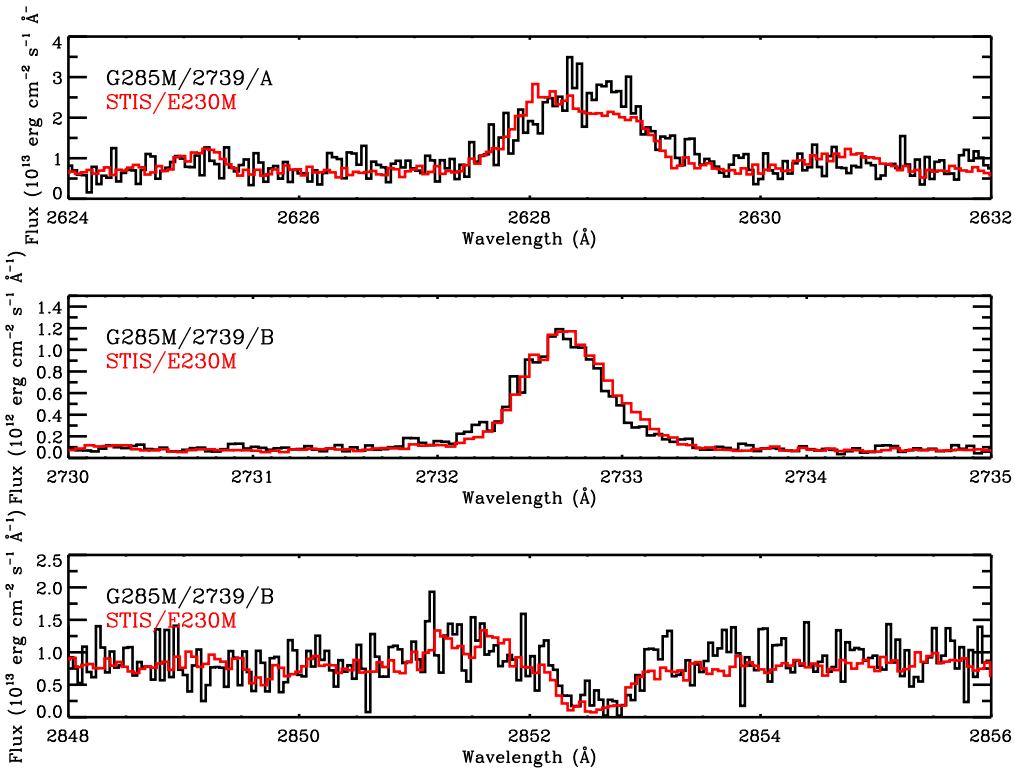

Figure 2. Comparison between STIS/E230M (red) and COS/G285M/2739 (black) wavelength scales using AG DRAC data. COS data is from program 11477, for FP-POS = 3.

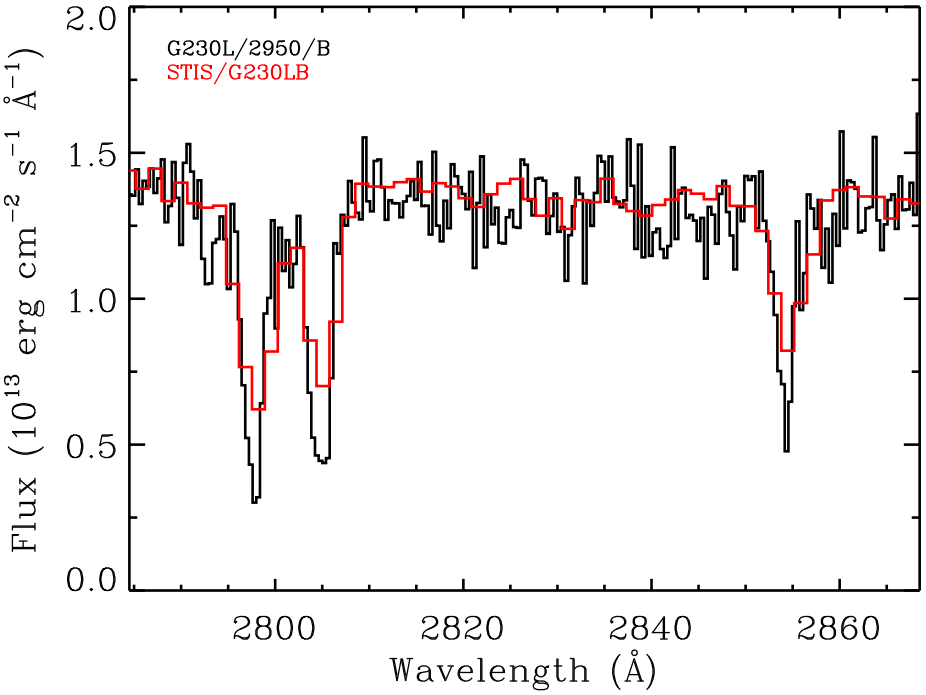

Figure 3. Comparison between STIS/G230LB (red) and COS/G230L/2950 (black) wavelength scales using AzV 18 data. COS data is from program 11472, for FP-POS = 3.